Molecular dynamics simulation of poly(3-hexylthiophene) helical structure in vacuo and in amorphous polymer surrounding

Journal Name

ARTICLE

Molecular dynamics simulation of poly(3-hexylthiophene) helical structure in vacuo and in amorphous polymer surrounding

Received 00th January 20xx,
Accepted 00th January 20xx

DOI: 10.1039/x0xx00000x

www.rsc.org/

N. I. Borzdun,[a] S. V. Larin,[b] S. G. Falkovich,[b] V. M. Nazarychev,[b] I. V. Volgin,[b] A. V. Yakimansky,[b] A. V. Lyulin,[c] V. Negi,[c] P. Bobbert[c] and S. V. Lyulin[b]

The stability of poly(3-hexylthiophene) (P3HT) helical structure has been investigated in vacuo and in amorphous polymer surrounding via molecular dynamics based simulations at temperatures below and above the P3HT melting point. The results show that the helical chain remains stable at room temperature both in vacuo and in amorphous surrounding, and promptly loses its structure at elevated temperatures. However, the amorphous surrounding inhibits the destruction of the helix at higher temperatures. In addition, it is shown that the electrostatic interactions do not significantly affect the stability of the helical structure.

1. Introduction

Solar energy is considered as one of the most promising sources of renewable energy. The use of photovoltaic cells has a number of significant advantages compared to other methods for solar power conversion. These include direct conversion of incident light into electricity, variety of component bases, as well as well-developed processing techniques.[1-3] However, there are some major shortcomings, in particular, the extreme toxicity of starting materials and high production costs of both the solar cells and power stations based on them.[4,5] Recent studies have suggested ways to overcome these limitations by developing new technologies such as using semiconducting conjugated polymers as the basis for organic photovoltaics.[6,7] Such solar cells are lightweight and flexible, their production involves the use of less toxic materials and it can be carried out using large scale roll-to-roll based processing techniques, resulting in substantial cost savings.

Regioregular poly(3-hexylthiophene) (P3HT) is a semiconducting conjugated polymer commonly used in organic electronics.[8-11] P3HT-based composites filled with fullerene C_{60} and its derivatives, such as phenyl-C_{61}-butyric acid methyl ester (PCBM), have proved to be one of the most promising materials for the production of organic photovoltaic cells.[12,13] The primary reason for this is the presence of a donor-acceptor interface between the polymer and PCBM components which leads to the formation of a bulk heterojunction based morphology. The efficiency of such solar cells essentially depends on the structure of polymer binder within the region of contacts with the filler. This is due to the fact that when introducing the filler into the polymer matrix, both materials must provide 'a continuous path' for electron and hole transport to the respective electrodes, to ensure efficient photocurrent generation.

The structure of a bulk P3HT sample is a combination of crystalline and amorphous domains, which is typical for semi-crystalline polymers. Conductivity is provided by crystalline regions, since the conjugation in these regions is ensured not only along the separate P3HT chains, but also between the neighbouring molecules. The most common representation of the P3HT crystalline domain structure is believed to be layers of parallel P3HT chains in elongated conformation.[14-17]

Formatting – please delete this box prior to submission

- Graphics, including tables, will be located at the top or bottom of the column following their first citation in the text during production (unless they are equations, which appear in the flow of the text). They can be single column or double column as appropriate and require appropriate captions.
- Text is not wrapped around any of the graphics.
- During production, sufficient space will be inserted around graphics for clarity of reading; a horizontal bar will also be used to separate all inserted graphics, tables and their captions from the text:

- Please consult the Styles menu for recommended formatting for all text, including footnotes, references, tables, images and captions.

However, Kiriy *et al.*[18] based on the detection of circulating currents, suggested the potential existence of the helical

[a] *Address here.*
[b] *Address here.*
[c] *Address here.*
† Footnotes relating to the title and/or authors should appear here.
Electronic Supplementary Information (ESI) available: [details of any supplementary information available should be included here]. See DOI: 10.1039/x0xx00000x

conformation of P3HT chains. Since the crystalline domain structure significantly affects the efficiency of organic solar cells, the present study aims to determine whether P3HT can exist in a helical conformation.

In the following section, the methodology of the implemented computer simulations is described, as well as the methods and the results from the model verification. The third section contains the comparison of the obtained results and their discussion. The main conclusions from this work are summarized in the last section.

2. Simulation details

We wish to probe the interactions between the polymer surrounding and an individual molecule present in the helical conformation and hence use an approach based on atomistic molecular-dynamics. Such simulations enable us to observe the time evolution of a single chain in a helical conformation and investigate the influence of temperature, electrostatic interactions and presence of the amorphous surrounding separately.

The inclusion of partial charges in the model and their influence on the stability of the macromolecular conformation represent separate tasks. Electrostatic interactions need not always be taken into account. Their effects strongly depend on the target properties of polymer systems. Even in the presence of strong polar groups, absence of the partial charges still correctly reproduces the structural properties of the studied systems, although it occasionally leads to incorrect determination of thermal characteristics.[19-21]

To investigate the stability of a P3HT chain in helical conformation, atomistic molecular dynamics simulation is performed using the GROMACS software package,[22,23] that is widely used for studying the structure and properties of polymers such as P3HT.[24,25] The structural formula of P3HT repeat unit is shown in Fig. 1.

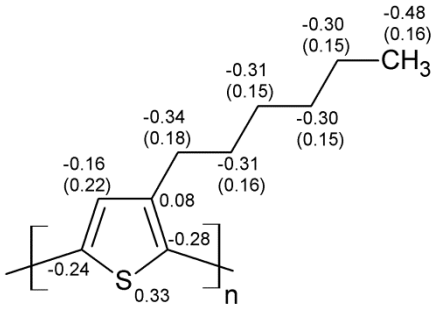

Fig. 1 The structure of the P3HT repeat unit. Numbers denote the partial atomic charges calculated for Gromos53a5 force field. Numbers in parentheses correspond to the partial charges of hydrogen atoms attached to the respective carbon atoms.

The initial helical conformation of a P3HT chain with degree of polymerization N_p = 70 is generated using the Build Polymer module of Materials Studio software package.[26] This degree of polymerization provides a sufficient number of turns within the helix. The angle of rotation between the monomer units is fixed at 0°, which enabled us to obtain a helical all-syn conformation similar to the structure proposed by Kiriy *et al.*[18] (Fig. 2). The energy of the initial chain configuration is minimized using the Discovery module of Materials Studio. The starting structures obtained after the energy minimization are then used to carry out the MD simulations.

Initially, a simulation box containing one P3HT helical chain in vacuo is set up. Then the chain is placed in an amorphous polymer surrounding, consisting of 27 P3HT molecules with a degree of polymerization N_p = 40 each. This degree of polymerization is large enough as it corresponds to the polymer regime and is routinely used in simulations.[27-29] The degree of polymerization of the P3HT chains in the amorphous phase is chosen to be lower than that of the helical chain, since a larger degree of polymerization leads to a significant increase in equilibration time of the amorphous surrounding and thus, increases the overall computational time. All our simulations are carried out using three-dimensional periodic boundary conditions.

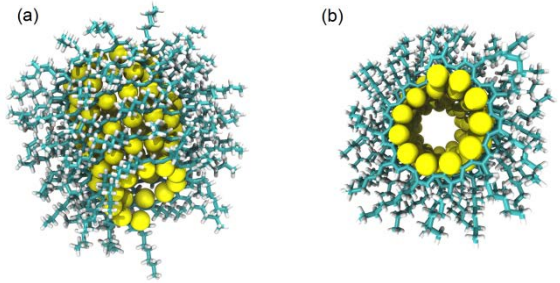

Fig. 2 The initial configuration of a P3HT helical chain: a) side view, b) top view.

The interactions in the systems under investigation are described by Gromos53a5,[30] OPLS-AA[31,32] and Amber99sb[33] force fields. The Gromos53a5 force field was selected due to its successful application to the simulations of heterocyclic polymers in our previous studies[19-21] whereas the OPLS-AA[34-36] and Amber[37-39] force fields are widely used in atomistic simulations of polythiophenes.

In all the force fields, potential energy is the sum of the bond stretching energy, the deformation energy of the bond angles and the angles of internal rotation, as well as the contributions responsible for the volume and electrostatic interactions. LINCS algorithm[40] is used to maintain the specified values of bond lengths, bond angles and angles of internal rotation. The electrostatic interactions are calculated using the PME method.[41,42]

Partial charges for P3HT atoms within the Gromos53a5 force field were calculated using the quantum-chemical Hartree-Fock method with basis set 6-31G* and Mulliken approach (HF/6-31G*(Mulliken)). The Hartree-Fock approach is the standard calculation method for the Gromos force field.[30] Furthermore, it has been shown via simulations of thermal properties of thermoplastic polyimides that the combination of this particular method with the Mulliken method for calculating the partial charges enables us to obtain the best agreement between computer simulations using the Gromos force field and experimental data.[20,21] The calculated values of the partial atomic charges are shown in Fig. 1. Partial charges for the OPLS-AA force field were taken from the atomistic model developed by Huang *et al.*[43] For the parameterization of electrostatic interactions in the Amber force field an applied quantum-chemical method HF/6-31G* (RESP), has been used.[44,45]

The MD simulations are carried out at a constant pressure of 1 atm and at three different temperatures: 300 K, 425 K, and 600 K. The P3HT melting point is about 513 K,[46-48] meaning that room temperature corresponds to the glassy state, and 600K corresponds to the melt. The temperature of 425 K was selected according to the thermal annealing protocol used in experiments for P3HT:PCBM blends.[49-50] The average temperature and pressure values are maintained at a constant value by employing the Berendsen thermostat and barostat with time constants $\boldsymbol{\tau_T}$ = 0.5 ps and $\boldsymbol{\tau_P}$ = 0.1 ps, respectively.[51]

In order to estimate the characteristic simulation time required to reach the equilibrium state and to verify the conformity of the simulation model with the real system, the simulation of the amorphous P3HT sample (the box containing 27 P3HT molecules consisting of 40 monomer units each) is carried out at 600 K. Randomly-coiled chains are distributed in a large enough cubic box followed by MD simulation for about 1.5 μs.

The time dependencies of the simulated chain mean-square end-to-end distance $\boldsymbol{H_{end-to-end}}$ and the radius of gyration $\boldsymbol{R_g}$ are shown in Fig. 3 for the systems without partial charges. Time dependencies of simulated $\boldsymbol{H_{end-to-end}}$ and $\boldsymbol{R_g}$ values calculated for the systems with electrostatic interactions differed very little from those obtained without electrostatic interactions.

Since these values reach a plateau after a simulation time of about 500 ns while using the Gromos53a5 force field, the system can be considered equilibrated after this simulation time. The values of $\boldsymbol{H_{end-to-end}}$ and $\boldsymbol{R_g}$ in case of the Amber force field reach the same level as in the Gromos53a5. However, for the OPLS-AA force field no significant changes in the size of the chains were observed during the whole simulation. Thus, it can be assumed that the system is almost 'frozen' even at a temperature of about 600 K while using the OPLS-AA force field indicating clearly that the model based on this force field describes the studied systems inadequately. To test the validity of this observation, a comparison of the calculated sizes of the chains and the values predicted theoretically was carried out.

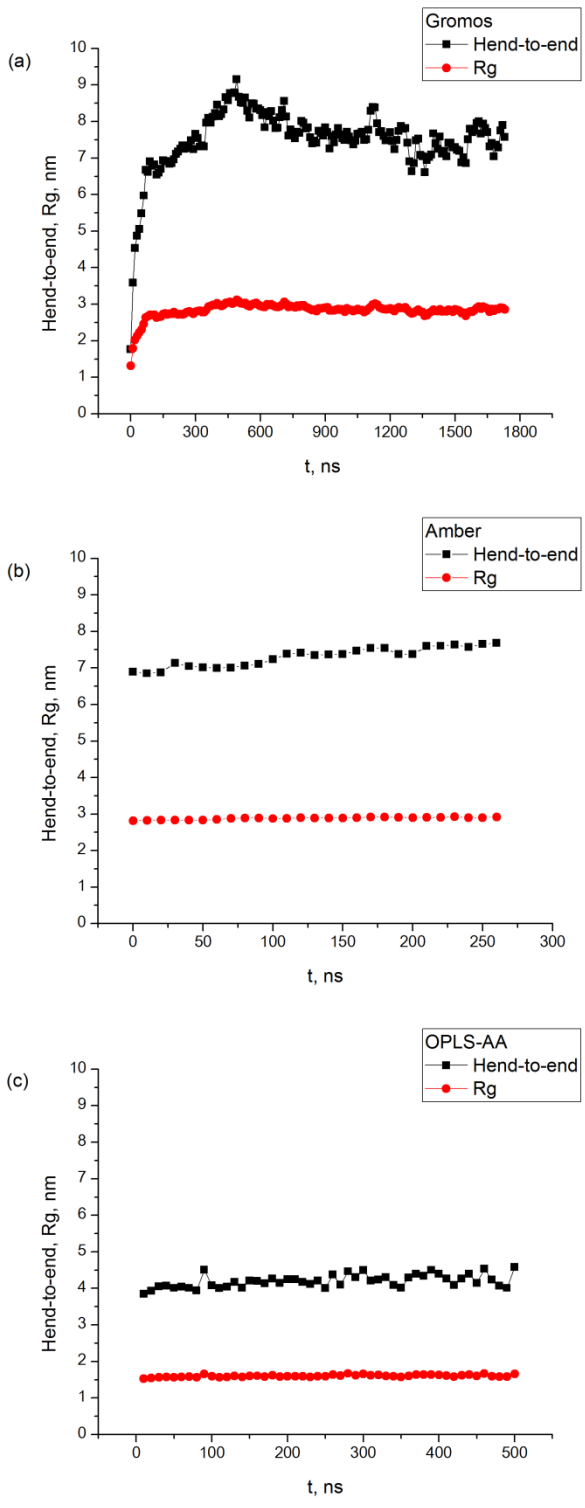

Fig. 3 Time dependence of the chain mean-square end-to-end distance ($\boldsymbol{H_{end-to-end}}$) and radius of gyration ($\boldsymbol{R_g}$) for the Gromos53a5 (a), Amber (b) and OPLS-AA (c) force fields without electrostatic interactions.

The estimated ratio of the squared average end-to-end distance to the squared average gyration radius $r_{sim} = \frac{H^2_{end-to-end}}{R^2_g}$ calculated after equilibration (see horizontal regions in Fig. 3) for the Gromos53a5, Amber and OPLS-AA force fields is very close to the value expected for a melt of infinitely long chains $r_{theor} = 6$.[52,53]

The persistence length and the Kuhn segment of P3HT chains were also calculated using a Kratky-Porod wormlike chain model. For chain sizes (the radius of gyration R_g and the end-to-end distance $H_{end-to-end}$), the contour (L) and persistence (l_p) lengths the following relations are well known:[54]

$$(1) < R_g^2 >= \frac{Ll_p}{3} - l_p^2 + \frac{2l_p^3}{L}\left[1 - \frac{l_p}{L} + \frac{l_p}{L}e^{-\frac{L}{l_p}}\right]$$

$$(2) < H^2_{end-to-end} >= 2l_pL\left(1 - \frac{l_p}{L}\left[1 - e^{-\frac{L}{l_p}}\right]\right)$$

We have calculated the contour length L = 15.4 nm of a P3HT chain with N_p = 40 degree of polymerization using the VMD visualization package. The average values of P3HT chain sizes obtained by averaging the instantaneous system configurations for the last 200 ns of simulation are represented in Table 1. In the Table the values of the persistence length and the Kuhn segment are also shown, calculated by substituting the obtained values of $\langle R_g^2 \rangle$ and $\langle H^2_{end-to-end} \rangle$ to equations (1) and (2), and by numerical solution of these equations for the Gromos53a5, Amber and OPLS-AA force fields. Comparison of these results with the experimental data, obtained by McCulloch *et al.* (A_{exp} = 6 ± 1 nm)[55] and Yakimansky *et al.* (A_{exp} = 6.0 ± 0.6 nm from rotational friction experiments and A_{exp} = 6.7 ± 0.7 nm from translational friction experiments),[56] suggests that the flexibility of P3HT chains is highly overestimated when using the OPLS-AA force field. This fact confirms the earlier assumption that the model based on this force field describes the studied systems inadequately. At the same time, for the Gromos53a5 force field, good agreement between the simulation results and the experimental data is observed. The values of the Kuhn segment obtained using the Amber force field are slightly lower as compared to the experimental values. Thus, the Gromos53a5 and Amber force fields were selected for the main part of the present study.

Table 1 Values of $< R_g^2 >$, $< H^2_{end-to-end} >$, the persistence length and the Kuhn segment of P3HT chains for the Gromos53a5, Amber and OPLS-AA force fields.

	$< R_g^2 >$, nm^2	$< H^2_{end-to-end} >$, nm^2	$l_p^{(1)}$, nm	$l_p^{(2)}$, nm	$A_{sim} = 2l_p$, nm
Gromos53a5	8.8	66.9	2.78	2.61	5.3 ± 0.2
Amber	8.4	54.8	2.05	2.55	4.3 ± 0.5
OPLS-AA	2.6	18.6	0.57	0.61	1.18 ± 0.04

The main simulation that is carried out after the verification of the model and selection of the force field consisted of several stages. First, simulation of the box containing one P3HT chain in a helical conformation in vacuo is performed without electrostatic interactions at T = 300 K (within 1 ns), T = 425 K (10 ps) and T = 600 K (10 ps). As it was mentioned above, the room temperature corresponds to the glassy state of P3HT, T = 600 K essentially exceeds the P3HT melting point of 513 K,[46-48] and the temperature of 425 K corresponds to when the annealing of P3HT:PCBM blends is carried out.[49-50] Then the P3HT helical structure is surrounded by 27 P3HT chains consisting of 40 monomer units each. In order to equilibrate the amorphous surrounding and alkyl 'tails' of the helix, simulation of the system was carried out at T = 600 K for 100 ns with a fixed position for the aromatic rings of the helix. Following that, simulation of helical structure with no constraints on the aromatic rings is performed in amorphous surrounding at temperatures of 300 K, 425 K, and 600 K respectively both with and without electrostatic interactions.

3. Results and discussion

From the MD simulations of a box comprising of one P3HT chain in helical configuration in vacuo using the Gromos53a5 force field, it is seen that at high temperatures (425 K and 600 K) the helical structure collapses within 10 ps of simulation, but at room temperature it remains stable for about 1 ns (Fig. 4).

Fig. 4 Typical snapshots of P3HT chains in vacuo after simulation using the Gromos53a5 force field at (a) 300 K for 1 ns, (b) 425 K for 10 ps, (c) 600 K for 10ps.

The P3HT chain surrounded by amorphous polymer retained its initial helical shape at 300 K for up to 1 μs of simulation using the Gromos53a5 force field (Fig. 5). At 425 K and 600 K, the helical structure collapsed, however, at 600 K the destruction occurred in less than 100 ns whereas at 425 K it took more than 100 ns. Since in vacuo the chain lost its helical shape in less than 10 ps, one can say that the amorphous surrounding effectively stabilizes the structure of the P3HT chain.

Fig. 5 Typical snapshots of P3HT chains in amorphous polymer surrounding after simulation using the Gromos53a5 force field at (a) 300 K for 1 μs, (b) at 425 K for 100 ns, (c) at 600 K for 100 ns without electrostatic interactions.

Similar simulations are carried out for the P3HT chain in a helical conformation in amorphous surrounding including electrostatic interactions. Typical snapshots of P3HT chain after 1 μs of simulation at 300 K and after 100 ns at 425 K and 600 K with and without electrostatic interactions indicate that they have no major difference (Fig. 6).

Fig. 6 Typical snapshots of simulated P3HT chains in amorphous polymer surrounding using the Gromos53a5 force field at (a) 300 K for 1 μs, (b) at 425 K for 100 ns, (c) at 600 K for 100 ns with electrostatic interactions.

For the P3HT chain in a helical configuration, the same simulation (in vacuo and in amorphous surrounding with and without electrostatic interactions) was performed using the Amber force field. It was found that after 250 ns of simulation at elevated temperatures of 425 K and 600 K with and without electrostatic interactions, the helical structure did not change substantially in comparison with the initial configuration. However, the temperature of 600 K significantly exceeds the P3HT melting point which is about 513 K,[46-48] thus suggesting the absence of any crystalline behavior. As a result, the accuracy of describing P3HT with the Amber force field requires additional investigation which is beyond the scope of this work. Therefore, we mainly focus on the results obtained using the Gromos53a5 force field.

3.1. Autocorrelation function $\boldsymbol{C(k)}$

For the numerical description of the destruction process of the P3HT helical structure, the autocorrelation function $\boldsymbol{C(k)}$[57] between the vectors connecting sulfur atoms separated by k repeating units of the chain (Fig. 7) has been calculated as

$$\boldsymbol{C(k)} = \frac{\mathbf{1}}{\boldsymbol{N-k}} \sum_{\boldsymbol{i=1}}^{\boldsymbol{N-k}} \frac{(\boldsymbol{d_i d_{i+k}})}{|\boldsymbol{d_i}||\boldsymbol{d_{i+k}}|}$$

where $\boldsymbol{d_i}$ is the vector connecting the $\boldsymbol{i}$th and $(\boldsymbol{i-1})$th sulfur atoms.

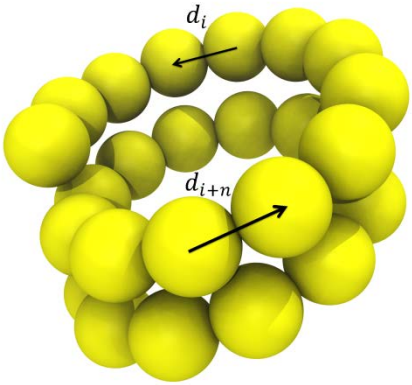

Fig. 7 The schematic representation of sulfur atoms from two turns of the helical P3HT chain. $\boldsymbol{d_i}$ are the vectors connecting the neighboring sulfur atoms in the chain.

Function $\boldsymbol{C(k)}$ is the average of the normalized inner product of the $\boldsymbol{i}$th and $(\boldsymbol{i+k})$th connecting vectors. The period of this function corresponds to the number of repeating units in a single turn of the helix. Increase in the period and decrease in the magnitude of the peaks at elevated temperatures display the changes in the helical structure.[57] As shown in Fig. 8, at the temperature of 300 K, $\boldsymbol{C(k)}$ does not undergo any changes during 100 ns of the simulation, both with and without electrostatic interactions, indicating the stability of the structure. Without electrostatic interactions, the peak heights are slightly reduced at 425 K. At 600 K, not only the heights of the maxima, but the period of the function $\boldsymbol{C(k)}$ varies significantly as well. Taking into account the electrostatic interactions at elevated temperatures of 425 K and 600 K, still leads to (less significant) changes in the period and height of the peaks. Thus, the inclusion of electrostatic interactions slightly inhibits the process of destruction of a helical structure.

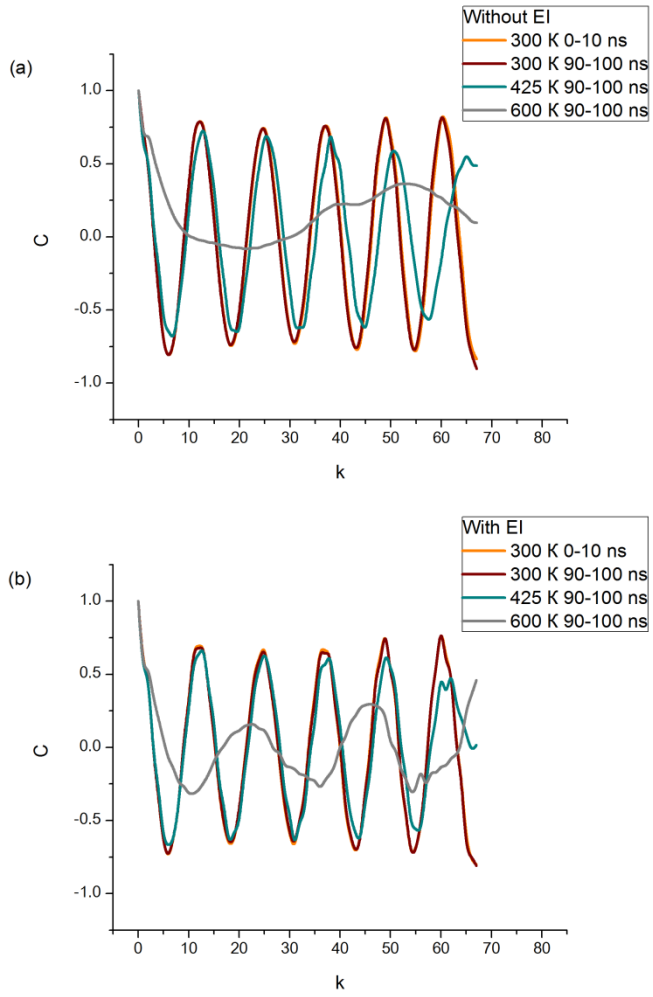

Fig. 8 The autocorrelation function $\boldsymbol{C(k)}$ calculated for P3HT chain in a helical conformation surrounded by the amorphous polymer at the beginning of simulation and after 100 ns of simulation at 300 K, 425 K and 600 K a) without and b) with electrostatic interactions.

Time dependence of the absolute values of $\boldsymbol{C(k)}$ averaged over intervals of 10 ns are also calculated (Fig. 9). The values of $\langle|\boldsymbol{C(k)}|\rangle$ are normalized to the initial value of the function $\boldsymbol{C_0(k)}$.

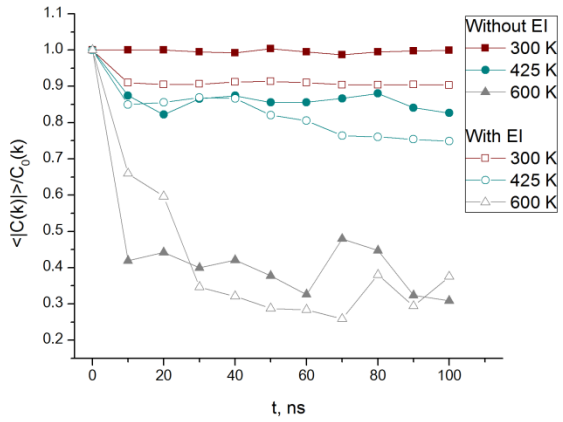

Fig. 9 Time dependence of $\langle|\boldsymbol{C(k)}|\rangle$ normalized to its initial value at 300 K, 425 K, and 600 K, calculated for systems with and without electrostatic interactions.

As shown in Fig. 9, the value of $\langle|\boldsymbol{C(k)}|\rangle$ remains constant during the simulation time at 300 K without including electrostatic interactions. At the same temperature of 300 K with electrostatic interactions, $\langle|\boldsymbol{C(k)}|\rangle$ still does not change with time, but the value of $\langle|\boldsymbol{C(k)}|\rangle$ is lower than that in the system without any electrostatic interactions. This difference may indicate a slight influence of partial charges on the spatial arrangement of the atoms within the helical chain. At elevated temperatures of 425 K and 600 K, a decrease in the value of $\langle|\boldsymbol{C(k)}|\rangle$ is observed that may be associated with the destruction of the helical structure.

3.1. Distribution of distances between nearest sulfur atoms $\boldsymbol{W(r)}$

To study the influence of partial charges on the stability of helical structure, the distance distribution between sulfur atoms from neighboring turns of P3HT chain in helical conformation has been investigated. First, the distances r between all the pairs of sulfur atoms from neighboring turns are calculated. Then, the normalized distribution of these distances $\boldsymbol{W(r)}$ is produced (Fig. 10).

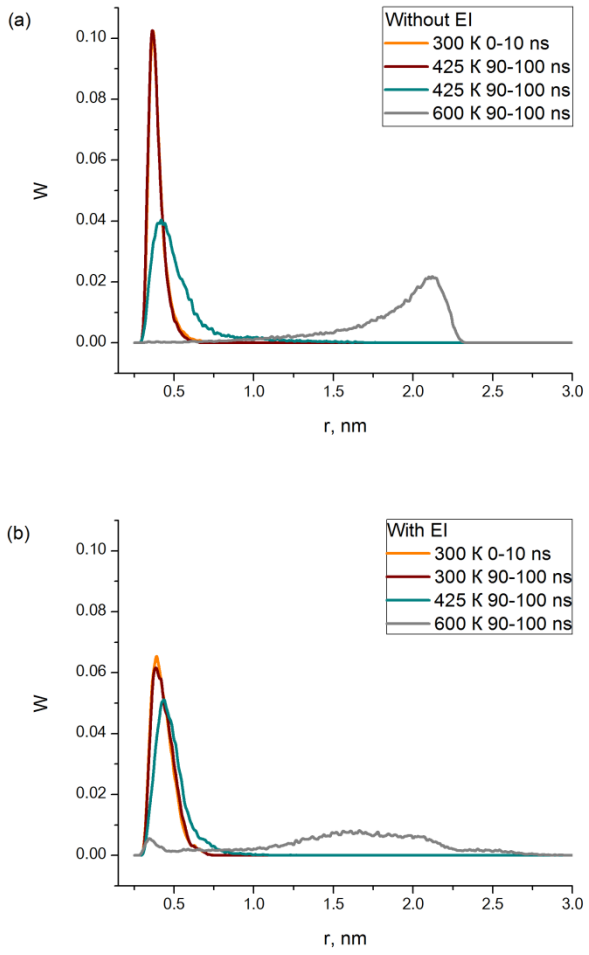

Fig. 10 The distribution of distances $W(r)$ between the nearest sulfur atoms for P3HT chain in a helical conformation at the beginning of simulation in amorphous surrounding and after 100 ns at 300K, 425K and 600K a) with and b) without electrostatic interactions.

The results obtained (Fig. 10) show that a P3HT chain in a helical conformation remains stable at room temperature and loses its shape at an elevated temperature of 600K within the simulation time. Despite the fact that the snapshots do not show any differences between the structure of the helix at 300 K and 425 K, the graphs clearly indicate that at 425K, the structure of the chain has become less stable, although it does not seem to undergo any visible change during 100 ns of simulation.

Conclusions

By means of atomistic molecular dynamics based simulations, the stability of P3HT helical structure is studied at room temperature of 300 K and at temperatures above (600 K) and slightly below (425 K) the P3HT melting point both in vacuo and in amorphous polymer surrounding, with and without electrostatic interactions.

The Kuhn length calculated using the OPLS-AA force field turned out to be small when compared to the values obtained from experimental studies. The Kuhn segment lengths obtained using the Gromos53a5 and Amber force fields are in good agreement with experiments. However, while using the Amber force field at temperature above the P3HT melting point, a 'frozen' structure is observed. Thus, the description of P3HT using the Gromos53a5 force field seems most appropriate.

P3HT helical structure remained stable at room temperature, regardless of the presence of the amorphous surrounding or addition of the electrostatic interactions. Increase in temperature has a significant effect on the stability of the structure: P3HT chain loses its helical shape at elevated temperatures of 425 K and 600 K. However, the destruction of the structure in the presence of the amorphous surrounding took a significantly longer time when compared to the vacuo simulations. Thus, the amorphous surrounding is able to inhibit the destruction of helical structure. The electrostatic interactions do not seem to substantially affect the stability of the P3HT helical structure.

Acknowledgements

This study has been supported by the Russian Foundation for Basic Research (grant № 15-03-07614). The simulations have been performed using the computational facilities of the Institute of Macromolecular Compounds, Russian Academy of Sciences, and the 'Chebyshev' and 'Lomonosov' supercomputers at Moscow State University.

Notes and references

‡
§
§§

1 J. Zaumseil and H. Sirringhaus. *Chem. Rev.*, 2007, **107**, 1296.
2 A. Facchetti. *Mater. Today*, 2007, **10**, 28.
3 R. N. Christopher, C. D. Frisblie, A. Demetrio, S. da Filho, J.-L. Brédas, P. C. Ewbank and K. R. Mann. *Chem. Mater.*, 2004, **16**, 4436.
4 C. D. Dimitrakopoulos and P. R. L. Malenfant. *Adv. Mater.*, 2002, **14**, 99.
5 M. Helgesen, R. Søndergaard and F. C. Krebs. *J. Mater. Chem.*, 2010, **20**, 36.
6 H. Hoppe and N. S. Sariciftci. *J. Mater. Res.*, 2004, **19**, 1924.
7 R. Kroon, M. Lenes, J. C. Hummelen, P. W. M. Blom and B. de Boer. *Polym. Rev.*, 2008, **48**, 531.
8 A. O. Patil, A. J. Heeger and F. Wudl. *Chem. Rev.*, 1998, **88**, 183.
9 Z. Bao, A. Dodabalapur and A. J. Lovinger. *Appl. Phys. Lett.*, 1996, **69**, 4108.
10 H. Sirringhaus, N. Tessler and R. H. Friend. *Science*, 1998, **280**, 1741.

11 H. Sirringhaus, P. J. Brown, R. H. Friend, M. M. Nielsen, K. Bechgaard, B. M. W. Langeveld-Voss, A. J. H. Spiering, R. A. J. Janssen, E. W. Meijer, P. Herwig and D. M. de Leeuw. *Nature*, 1999, **401**, 685.
12 S. Gunes, H. Neugebauer and N. S. Sariciftci. *Chem. Rev.*, 2007, **107**, 1324.
13 H. Zhu, J. Wei, K. Wang and D. Wu. *Sol. Energ. Mat. Sol. C.*, 2009, **93**, 1461.
14 J. M. Y. Carrillo, R. Kumar, M. Goswami, B. G. Sumpter and W. M. Brown. *Phys. Chem. Chem. Phys.*, 2013, **15**, 17873.
15 K. Rahimi, I. Botiz, N. Stingelin, N. Kayunkid, M. Sommer, F. P. V. Koch, H. Nguyen, O. Coulembier, P. Dubois, M. Brinkmann and G. Reiter. *Angew. Chem. Int. Edit.*, 2012, **51**, 11131.
16 K. Rahimi, I. Botiz, J. O. Agumba, S. Motamen, N. Stingelin and G. Reiter. *RSC Adv.*, 2014, **4**, 11121.
17 W. Hourani, K. Rahimi, I. Botiz, F. P. V. Koch, G. Reiter, P. Lienerth, T. Heiser, J. L. Bubendorff and L. Simon. *Nanoscale*, 2014, **6**, 4774.
18 N. Kiriy, E. Jähne, H. J. Adler, M. Schneider, A. Kiriy, G. Gorodyska, S. Minko, D. Jehnichen, P. Simon, A. A. Fokin and M. Stamm. *Nano Lett.*, 2003, **3**(6), 707.
19 S. V. Larin, S. G. Falkovich, V. M. Nazarychev, A. A. Gurtovenko, A. V. Lyulin and S. V. Lyulin. *RSC Adv.*, 2014, **4**, 830.
20 S. G. Falkovich, S. V. Lyulin, V. M. Nazarychev, S. V. Larin, A. A. Gurtovenko, N. V. Lukasheva and A. V. Lyulin. *J. Polym. Sci. Pol. Phys.*, 2014, **52**, 640.
21 V. M. Nazarychev, S. V. Larin, A. V. Yakimansky, N. V. Lukasheva, A. A. Gurtovenko, I. V. Gofman, V. E. Yudin, V. M. Svetlichnyi, J. M. Kenny and S. V. Lyulin. *J. Polym. Sci. Pol. Phys.*, 2015, **53**, 912.
22 B. Hess, C. Kutzner, D. van der Spoel and E. Lindahl. *J. Chem. Theory Comput.*, 2008, **4**(3), 435.
23 D. van der Spoel, E. Lindahl, B. Hess, G. Groenhoff, A. E. Mark and H. J. C. Berendsen. *J. Comput. Chem.*, 2005, **26**(16), 1701.
24 Y. Takizawa, T. Shimomura and T. Miura. *J. Phys. Chem. B*, 2013, **117**, 6282.
25 S. Obataz and Y. Shimoi. *Phys. Chem. Chem. Phys.*, 2013, **15**, 9265.
26 Materials Studio, http://accelrys.com/products/materials-studio, (accessed June 2016).
Accelrys Software Inc., San Diego. Note that some of these codes were also offered as part of the Cerius 2 application that preceded Materials Studio. 2013. Available from http://accelrys.com/products/materials-studio/
27 T. Liu, D. L. Cheung and A. Troisi. *Phys. Chem. Chem. Phys.*, 2011, **13**, 21461.
28 M. Bernardi, M. Giulianini and J. C. Grossman. *ACS Nano*, 2010, **4**(11), 6599.
29 Y. Yimer and M. Tsige. *J. Chem. Phys.*, 2012, **137**, 204701.
30 C. Oostenbrink, A. Villa, A. E. Mark and W. F. van Gunsteren. *J. Comput. Chem.*, 2004, **25**(13), 1656.
31 W. L. Jorgensen, D. S. Maxwell and J. Tirado-Rives. *J. Am. Chem. Soc.*, 1996, **118**, 11225.
32 D. S. Maxwell, J. Tirado-Rives and W. L. Jorgensen. *J. Comput. Chem.*, 1995, **16**, 984.
33 J. Wang, R. M. Wolf, J. W. Caldwell, P. A. Kollman and D. A. Case. *J. Comput. Chem*., 2004, **25**, 1157.
34 K. N. Schwarz, T. W. Kee and D. M. Huang. *Nanoscale*, 2013, **5**, 2017.
35 C. Poelking and D. Andrienko. *Macromolecules*, 2013, **46**, 8941.
36 N. R. Tummala, C. Bruner, C. Risko, J.-L. Brédas and R. H. Dauskardt. *ACS Appl. Mater. Interfaces*, 2015, **7**, 9957.
37 E. F. de Oliveira and F. C. Lavarda. *J. Polym. Sci. Pol. Phys.*, 2013, **51**, 1350.
38 M. I. Saba and A. Mattoni. *J. Phys. Chem. C.*, 2014, **118**, 4687.
39 G. D'Avino, S. Mothy, L. Muccioli, C. Zannoni, L. Wang, J. Cornil, D. Beljonne and F. Castet. *J. Phys. Chem. C.*, 2013, **117**, 12981.
40 B. Hess, H. Bekker, H. J. C. Berendsen and J. G. E. M. Fraaije. *J. Comput. Chem*., 1997, **18**(12), 1463.
41 T. Darden, D. York and L. Pedersen. *J. Chem. Phys*. 1993, **98**(12), 10089.
42 U. Essmann, L. Perera, M. L. Berkowitz, T. Darden, H. Lee and L. G. Pedersen. *J. Chem. Phys.*, 1995, **103**(19), 8577.
43 D. M. Huang, R. Faller, K. Do and A. J. Moulé. *J. Chem. Theory Comput.*, 2010, **6**(2), 527.
44 J. Wang, P. Cieplak and P. Kollman. *J. Comput. Chem.*, 2000, **21**, 1049.
45 A. Jakalian, B. Bush, D. Jack and C. Bayly. *J. Comput. Chem*., 2002, **23**, 1623.
46 C. Müller, T. A. M. Ferenczi, M. Campoy-Quiles, J. M. Frost, D. D. C. Bradley, P. Smith, N. Stingelin-Stutzmann and J. Nelson. *Adv. Mater.*, 2008, **20**, 3510.
47 J. Zhao, A. Swinnen, G. V. Assche, J. Manca, D. Vanderzande and B. Van Mele. *J. Phys. Chem. B.*, 2009, **113**, 1587.
48 Y. Zhao, G. Yuan, P. Roche and M. Leclerc. *Polymer*, 1995, **36**(11), 2211.
49 W. Yin and M. Dadmun. *ACS Nano*, 2011, **5**, 4756.
50 D. Chen, F. Liu, C. Wang, A. Nakahara and T. P. Russell. *Nano Lett.*, 2011, **11**, 2071.
51 H. J. C. Berendsen, ed. M. Meyer and V. Pontikis, *Computer Simulation in Materials Science,* Kluwer Academic Publ., Dordrecht, 1991.
52 P. J. Flory, *Statistical mechanics of chain molecules*, Wiley-Interscience, New York, 1969.
53 T. Vettorel and K. Kremer. *Macromol. Theor. Simul.*, 2010, **19**, 44.
54 H. Benoit and P. Doty. *J. Phys. Chem.,* 1953, **57**, 958.
55 B. McCulloch and V. Ho. *Macromolecules*, 2013, **46**, 1899.
56 A. V. Yakimansky, S. V. Bushin, M. A. Bezrukova, A. A. Lezov, A. S. Gubarev, E. V. Lebedeva, L. I. Akhmadeeva, A. N. Podseval'nikova, N. V. Tsvetkov, G. Koeckelberghs and A. Persoons. *J. Polym. Sci. Pol. Phys.*, 2016, DOI: 10.1002/polb.23986.
57 M. K. Glagolev, V. V. Vasilevskaya and A. R. Khokhlov. *Polym. Sci. Ser. A*, 2010, **52**(7), 761.